Tailoring Morphologies in Polymeric High Internal Phase Emulsions by Selective Solvent Casting

Raffaele Mezzenga,[†] Glenn H. Fredrickson,[†,‡] and Edward J. Kramer*[,†,‡]

Materials Department, University of California, Santa Barbara, California 93106, and Department of Chemical Engineering, University of California, Santa Barbara, California 93106

Received July 25, 2002

ABSTRACT: A wide range of different morphologies have been obtained by solvent casting of mixtures of polystyrene (PS) and poly(2-vinylpyridine) homopolymers (PVP) with PS−PVP block copolymer. The curvature of the PS−PVP interface has been investigated as a function of polymer molecular weights, solvent quality, and blend composition. For blends with highly asymmetric composition at equilibrium, simulations based on self-consistent-field theory (SCF) predicted a curvature of the interface toward the minority phase. Casting PS/PVP blends from a common solvent for both PS and PVP resulted in morphologies that were in qualitative agreement with SCF simulations. These morphologies nucleated and grew from an initially fully homogeneous solution. Quite different morphologies resulted when mixtures of separate solutions of PS and PVP in selective solvents were cast, if PS−PVP of the appropriate asymmetry was added to either the PS or PVP solution. Polymeric high internal phase emulsions (polyHIPE) were formed in which the majority phase was dispersed in the continuous minority phase. A requirement for successful polyHIPE formation is that the selective solvent for the homopolymer and majority block of the block copolymer (continuous phase of the polyHIPE) has to be a sufficiently poor solvent for the minority block, thus inducing a strong segregation of the block copolymer at the interface between the two solution phases. A simple way to ensure that this condition is satisfied is to verify that the PS−PVP block copolymers form micelles in the selective solvents. The formation of such micelles was detected using dynamic light scattering.

Introduction

The equilibrium morphology of a blend formed by mixing homopolymers depends essentially on the temperature and composition of the blend. For immiscible polymers, the equilibrium state is achieved by minimizing the total free energy associated with the formation of interfaces. Since the interfacial tension between two highly immiscible polymers depends primarily on the Flory−Huggins interaction parameter between segments with small corrections for finite molecular weights,[1−3] this means that, once these parameters have been fixed, equilibrium is achieved by minimizing the total interfacial area, subject to constraints on the relative phase volumes. While not a true equilibrium, but rather a metastable equilibrium, it is usually observed that the polymer present at lower volume fraction is dispersed in the form of droplets within a continuous phase formed by the other polymer. The introduction of a block copolymer as a third component leads to more complex cases. In particular, as widely discussed in the literature, asymmetric diblock copolymers may impart an intrinsic curvature to a flat interface, bending the interface toward the shorter block.[4−6] Thus, if the homopolymer present in larger concentration is also that forming the shorter block of the copolymer, two competing effects will drive the final curvature of the interface. In this case, approximate analytical theories or self-consistent-field theory can be used to predict the final curvature of the interface.[5,7]

Strict equilibrium conditions are, in general, extremely difficult to realize in practice, and nonequilibrium procedures normally have to be used in order to invert the curvature of the interface and maintain continuity in the minority phase. The procedure most widely used is similar to the emulsification process of water/oil/surfactant systems.[8−10] In those systems, high internal phase emulsions (HIPE) with a dispersed oil phase volume fraction as high 90% can be obtained by adding the oil phase dropwise to the water/surfactant solution under continuous stirring.[11−15] In the case of polymeric systems, emulsions of similar phase volume fractions can be obtained by a multistep procedure. Petroleum ether or another low molecular weight species is dispersed dropwise in a solution containing monomer, normally styrene or divinylbenzene, solvent, and surfactant.[16−19] The subsequent steps consist of the free radical polymerization of the continuous monomer phase and the removal of the solvent. The resulting compositions consist of a polymeric network and a low molecular weight dispersed phase. Structural or mechanical applications of these blends are thus rather limited, and the dispersed phase is usually removed to produce foams with very low density.[20−25] True polymeric high internal phase emulsions (polyHIPE), where both polymeric phases are synthesized by similar techniques, would require an additional step to polymerize the dispersed phase.

These blends are of interest in a range of applications. For example, a miscible, doped π-conjugated polymer could be added to the percolating phase, thus conferring a low level of electrical conductivity needed for antistatic or corrosion protection applications at moderate cost. Alternatively, the percolating phase could be made ion conducting so that the blend could serve as a separator membrane for battery applications. Where transport of certain molecules must be limited, an expensive polymer with excellent barrier properties could be employed as the minor continuous phase and combined with a discontinuous, inexpensive polymer with good mechanical properties.

[†] Materials Department.
[‡] Department of Chemical Engineering.
* To whom correspondence should be addressed: e-mail edkramer@mrl.ucsb.edu, Tel + 1 805 893 4999, Fax + 1 805 893 8486.

10.1021/ma021196l CCC: $25.00
Published on Web 05/23/2003

Table 1. Molecular Weight of Homopolymers and Copolymers

homopolymer	M_w (g/mol)	homopolymer	M_w (g/mol)	copolymer	M_w (g/mol)
PS_1	9 000	pVP_1	8 000	$PS-PVP_1$	70 000
PS_2	35 000	pVP_2	42 000	$PS-PVP_2$	100 000
PS_3	120 000	pVP_3	140 000		

In the present work, we discuss a different procedure to produce polyHIPE from premade homopolymers and block copolymers, whose emulsification based on selective solvent casting does not require any polymerization process. Although a wide range of morphologies can be obtained by solvent casting,[26−29] we will show that only a specific selection of solvents, copolymers, and homopolymer molecular weights leads to the production of polyHIPE blends. In particular, it will be demonstrated that a suitable emulsion process leads to metastable polyHIPE morphologies in which the high internal phase volume ratio is well beyond that of close packing of spherical domains of the discrete phase. The conditions under which this emulsification process occurs will be elaborated on.

Experimental Section

Materials. Polystyrene (PS) and poly(2-vinylpyridine) (PVP) constitute a good model system for the study, owing to their high immiscibility, similar density (1.04 g/mL), and nearly matched repeat unit molecular weight (PS = 104 g/mol, PVP = 105 g/mol). Narrow molecular weight distribution polystyrenes, with M_w = 9000, 35 000, and 120 000 g/mol, were purchased from Pressure Chemicals and are identified in the following by PS_1, PS_2, and PS_3, respectively. Poly(2-vinylpyridines) with M_w = 8000, 42 000, and 140 000, designated as PVP_1, PVP_2, and PVP_3, respectively, were synthesized by anionic polymerization according to procedures described elsewhere.[30] Two different PS−PVP diblock copolymers were synthesized. The first, $PS-PVP_1$, had a M_w = 70 000 g/mol and a PVP volume fraction, f_{PVP}, of 0.84, determined from the nitrogen content as obtained by elemental analysis.[30] The second, $PS-PVP_2$, had M_w = 114 000 g/mol, with f_{PVP} = 0.13. In all the compounds used, the polydispersity (M_w/M_n) was lower than 1.1. Table 1 summarizes the molecular weights of the polymers used. Several solvents, chloroform, ethanol, toluene, and cyclohexane, were selected and used as received from Aldrich.

Procedures. *Self-Consistent-Field Theory.* Self-consistent-field theory was implemented in two dimensions using the algorithm described by Drolet and Fredrickson.[31] Numerical simulations of incompressible ternary blends of PS homopolymer, PVP homopolymer, and PS−PVP diblock copolymer were carried out for a variety of molecular weights and compositions. The Flory−Huggins χ parameter between PS and PVP segments was fixed at a value of 0.11, and periodic boundary conditions were employed. Initial conditions for the simulations were disordered chemical potential field patterns produced with a random number generator. Calculations were done using a 120 × 120 lattice of L = 18 (units of copolymer radius of gyration). The contour integration step was fixed at Δs = 0.2. The potential fields were updated until stable or metastable structures were obtained.

Blend Preparation. The blends investigated had in all cases a high volume fraction of one homopolymer and a low fraction of the other polymer and copolymer. High PS volume fraction blends were prepared as follows: each PVP homopolymer was dissolved together with $PS-PVP_1$ in a good solvent for PVP to form a 20 wt % polymer (PVP plus $PS-PVP_1$) solution. This composition is similar to the monomer plus surfactant solutions used for producing polyHIPE foams.[19,20] PS was then dissolved in a separate good solvent for PS, either toluene at room temperature or cyclohexane at 50 °C. This solution was then added to the PVP/copolymer/solvent solution dropwise, under continuous stirring at 200 rpm. To avoid phase inversion during emulsification, the volume of the PS/solvent solution had to be minimized as compared to that of PVP/ $PS-PVP_1$/ solvent. Thus, a polymer concentration of 50 wt % was selected for the PS/solvent solution. The solution was stirred for 10 min. Then solvent was removed by a combination of vacuum and gentle heating: vacuum at room temperature was applied first, then the mixture was heated at 60 °C under atmospheric pressure, and finally vacuum was applied at 90 °C for 30 min. This procedure avoided bubble formation during solvent removal. High PVP volume fraction blends were obtained by mixing PVP, PS, and $PS-PVP_2$, following a similar procedure. PS was dissolved together with $PS-PVP_2$ in a good solvent for PS to form a 20 wt % polymer (PS plus $PS-PVP_2$) solution. PVP was then dissolved in a separate good solvent for PVP to form a 50 wt % polymer solution. The latter mixture was finally added to the PS/copolymer/solvent solution dropwise, under continuous stirring at 200 rpm that was maintained for 10 min. The solvent was finally removed as described previously. The final volume fractions of the dry blends were 0.13, 0.07, and 0.8 for the minority homopolymer, the block copolymer, and the majority homopolymer, respectively.

Transmission Electron Microscopy (TEM). The 100 nm thick films of the final blends were microtomed with a Leica Ultra Cut microtome. The PVP phase was stained for 6 h at 25 °C in saturated I_2 vapor above solid I_2. Micrographs of the final morphologies were taken using a JEOL2000FX transmission electron microscope operated at 200 kV.

Light Scattering. Light scattering experiments were performed using a Brookhaven Instruments system with detector set at an angle of 90° to minimize reflection effects. The block copolymers were dissolved in different solvents at various concentrations and temperatures. Concentrations ranging between 0.01 and 0.5 g/mL were used at temperatures ranging between room temperature and 50 °C. The micelle size results were extrapolated to zero concentration to avoid effects from interactions among micelles as well as multiple light scattering.

Results and Discussion

In all the blends investigated in this work, the interface curvature is, as anticipated in the Introduction, the result of two opposite driving forces: the asymmetry of the block copolymer, which tends to bend the interface toward the shorter block, and the high asymmetry of the blend composition, which tends to favor morphologies with the opposite curvature. If the concentration of the block copolymer and the interaction parameter are maintained fixed, the curvature of the PS/PVP interface at equilibrium will only be a function of the homopolymer composition of blend. Figure 1 shows the self-consistent theory predictions of the interface curvature for two different cases of PVP/PS/PS−PVP1 systems as a function of blend composition. The Flory−Huggins interaction parameter is fixed at 0.11, which for PS/PVP corresponds to a temperature of 170 °C, at which PS/PVP blends are in the melt state.[30] Note that the morphologies shown in Figure 1 should be viewed as metastable rather than true equilibrium structures.

The concentration of block copolymer, $PS-PVP_1$, is maintained fixed at 7% in both parts a and b of Figure 1. In Figure 1a, the light regions correspond to higher concentrations of PVP_1 while the dark regions correspond to PS_2-rich domains. The block copolymer is located at the interface. The conditions of wet brush on the PVP side of the interface and dry brush on the PS side lead to a phase inversion at a volume fraction of PVP between 33% and 38%. The opposite case is illustrated in Figure 1b. The conditions are dry brush on the PVP side of the interface and wet brush on the PS side. Thus,

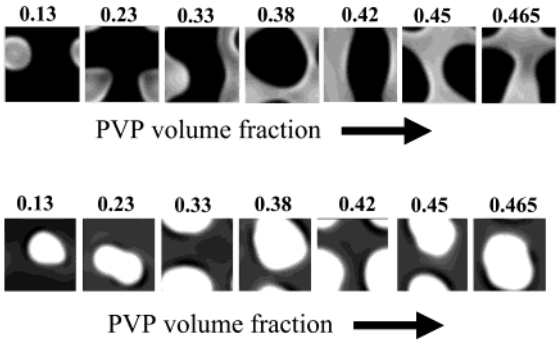

Figure 1. Self-consistent theory predictions of the interface curvature as a function of blend composition and polymer molecular weights. The concentration of block copolymer, PS−PVP_1, is 7% in the two cases. **(**a, top**)** Light color is PVP_1 (M_w = 8000 g/mol); dark is PS_2 (M_w = 35 000 g/mol). The conditions of wet brush in the PVP block and dry brush in the PS blocks lead to a phase inversion at a composition of 33−38% PVP. **(**b, bottom**)** Light color is PVP_3 (M_w = 140 000 g/mol); dark is PS_1 (M_w = 9000 g/mol). The conditions of dry brush in the PVP block and wet brush in the PS block cause the PS to remain as the continuous phase at the different compositions investigated.

the curvature of the interface is toward the PVP phase, and PS is the continuous phase at all compositions up to the symmetric composition of 0.465/0.465 PS/PVP. Since the polyHIPEs targeted in the present work are required to have an internal phase volume fraction above 74%, the SCF simulations show that, with the polymers selected, it is not possible to realize stable polyHIPE. Nevertheless, SCF simulations constitute a valuable input for defining an appropriate system for producing a polyHIPE. Indeed, we shall see for a system similar to that simulated in Figure 1a phase inversion may be induced at even lower PVP volume fractions, if nonequilibrium processes are employed.

A first attempt to produce blends of the same compositions as those shown in Figure 1a was done by solvent casting from homogeneous solutions of PS, PVP, and PS−PVP. In solution, the three components can be assumed to be at equilibrium, but the development of the morphology during solvent removal is a nonequilibrium process. However, if the removal of the solvent is relatively slow, as for the blends prepared in the present work, one can assume that the curvature of the interface will approach that predicted on the simulations. In this respect, Figure 2 shows the morphology of a $PVP_1/PS_2/PS-PVP_1$ blend of composition 0.13/0.80/0.07 respectively, by volume, as obtained by using chloroform as a common solvent for both PS and PVP. The mixing procedure is described in the Experimental Section. Owing to the high asymmetry in blend composition, the minority phase, which is the dark stained PVP, is dispersed in the form of droplets within a continuous majority phase (PS). This is in agreement with the predictions of the self-consistent theory simulations (see blend of composition 0.13 in Figure 1a). Nevertheless, a more complex morphology is observed in the real case, with small submicrometer PS droplets being present within the PVP larger particles, whereas SCF calculations within a box of nanometer dimensions identified only one size scale of droplets.

To invert the curvature of the main interface and maintain the same composition of the blend, it is therefore necessary to follow a nonequilibrium procedure. A possible method is to use selective solvents for PS and PVP. A second $PVP_1/PS_2/PS-PVP_1$ blend of the same composition as that shown in Figure 2 was cast by first dissolving PVP_1 and PS−PVP_1 in ethanol and then adding (dropwise) PS_2 dissolved in toluene. After separate solutions are made, the process is identical to that described in the Experimental Section. Ethanol has been selected because it is a nonsolvent for PS whereas toluene is a nonsolvent for PVP but a good solvent for PS. This will decrease the solubility of the PS solution in the PVP−copolymer solution, and eventually, an emulsion can be obtained, where droplets of the PS solution will be wetted by the PVP/PS−PVP/ethanol solution. The nature of the emulsion obtained by following this procedure is demonstrated in Figure 3a, which shows an optical micrograph of the blend after 10 min of continuous stirring. A TEM micrograph of the same blend after solvent removal, shown in Figure 3b, proves more clearly the polyHIPE nature of the blend. Remarkably, the minority phase, PVP, is maintained as a continuous network, whereas the majority phase, PS, is dispersed as large droplets. This is in contrast with the usual phase inverted morphology at such a composition. However, the curvature of the PS/PVP interface is consistent with the block copolymer asymmetry. There is also no residual trace of any secondary phase separation within the PS droplets, indicating a poor mixing of the PS and PVP solutions. This suggests that in the final dry blend the block copolymer is primarily located at the interfaces between the two phases evident in Figure 3b.

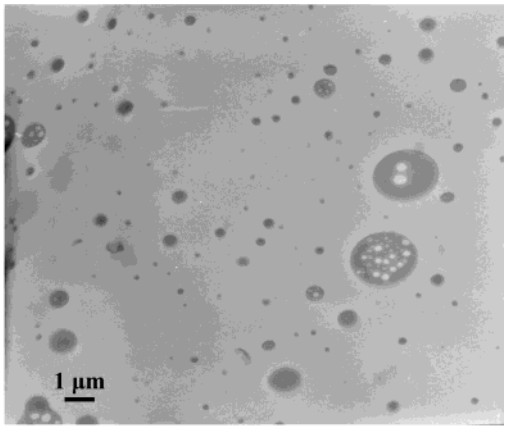

Figure 2. TEM micrograph of $PVP_1/PS_2/PS-PVP_1$ blend of composition by volume, 0.13/0.80/0.07, respectively, as obtained from solvent casting using chloroform as common solvent for PVP and PS.

The conditions of stability of this interfacial curvature can be explored by changing the composition of the blend and the molecular weights of the two homopolymers in contact with the two blocks of the copolymer at the interface, as done previously for the SCF simulations. The volume fraction of PVP was further reduced in order to establish the limit to which this phase could be maintained continuous and the PS dispersed. However, a modest decrease in the volume fraction of PVP resulted in a loss of network continuity. Figure 4 shows the illustrative case of a $PVP_1/PS_2/PS-PVP_1$ blend with composition 0.10/0.84/0.06, respectively, by volume. The coexistence of some discontinuous PS domains with PVP ones and the elongated shape of the PVP discontinuous domains constitute further evidence of the deviation from equilibrium morphologies, since the minimization of the total interfacial energy requires spherical dispersed domains of the minority phase.

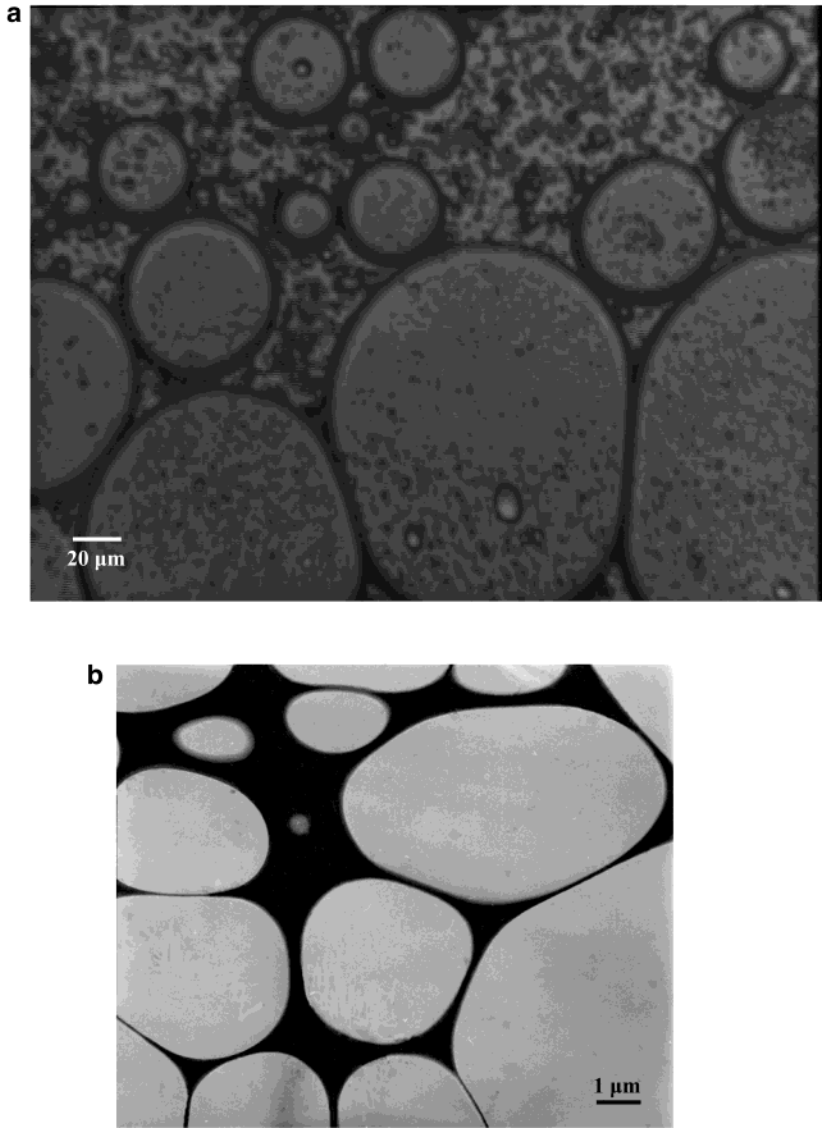

Figure 3. $PVP_1/PS_2/PS-PVP_1$ blend of composition 0.13/0.80/0.07 by volume, respectively, as obtained from solvent casting using ethanol as solvent for PVP plus $PS-PVP_1$ and toluene for PS. **(**a**)** Optical micrograph prior to solvent removal. **(**b**)** TEM micrograph of dried blend. The droplets (PS) and the continuous phase (PVP) of the optical micrograph (a), swollen by toluene and ethanol, respectively, are precursors of the final dispersed (PS) and continuous (PVP) phases of the dried blend (b).

The effects of wet or dry brush conditions for block copolymer/homopolymer interfaces, observed in dried blends, have been explored on both sides of the block copolymer, for a fixed $PVP/PS/PS-PVP_1$ blend composition of 0.13/0.80/0.07. When the block copolymer/PVP_1 interface was a wet brush and the copolymer/PS_2 or PS_3 interface a dry brush, a continuous PVP network was maintained throughout the whole sample indicative of good interfacial stability (see Figure 3b). This is consistent with the fact that a homopolymer with a molecular weight lower than the block swells the block and contributes to bending the interface toward the opposite side of the block copolymer at the interface. On the other hand, dry brush conditions on the continuous PVP_3 side of the interface or wet brush conditions on the discontinuous PS_1 side resulted in a polyHIPE blend, but with a loss of long-range PVP network continuity. A typical example is pictured in Figure 5, which shows a TEM micrograph of the dried $PVP_3/PS_1/PS-PVP_1$ blend.

Following the same strategy, attempts to prepare a 0.13/0.80/0.07 $PS_1/PVP_2/PS-PVP_2$ blend were made by dissolving PS_1 and $PS-PVP_2$ in toluene and adding

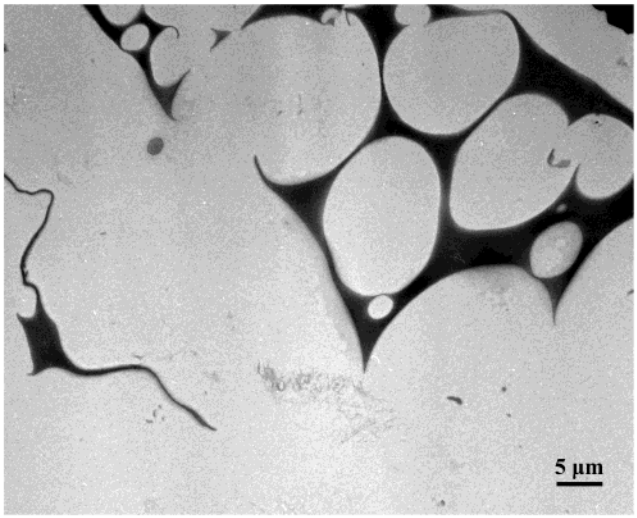

Figure 4. TEM micrograph showing loss of PVP network continuity for a blend of $PVP_1/PS_2/PS-PVP_1$ at a composition 0.10/0.84/0.06, respectively, by volume.

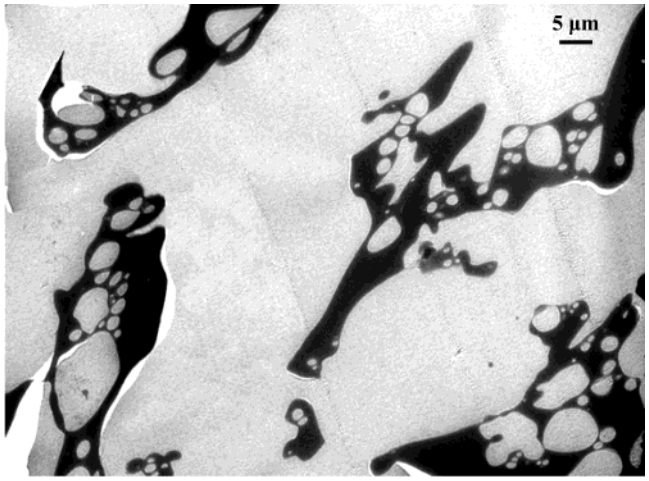

Figure 5. TEM micrograph of dried $PVP_3/PS_1/PS-PVP_1$ blend of composition 0.13/0.80/0.07 by volume, respectively, as obtained from solvent casting using ethanol as solvent for PVP and toluene for PS. The dry/wet brush conditions in the PS/PVP phases at the interface lead to a breaking up of the PVP network continuity.

dropwise the solution of PVP_2 and ethanol, at the concentrations described in the previous cases. Surprisingly, emulsification did not occur in this system, as was shown by both by optical and TEM microscopy (Figure 6, a and b, respectively). The final morphology resulted in a continuous phase formed by the majority phase (PVP), and the lower volume fraction of PS was observed in the form of dispersed droplets. Furthermore, TEM revealed the presence of small particles of PVP within the PS droplets, suggesting, similar to the case of the blend of Figure 1, that a more extended mixing of components occurred during the blending procedure. The main difference between this blend and that of Figure 3 is in the solubilities of the different polymers in the two solvents selected. The solubility and surfactant characteristics of the two copolymers in the two solvents are also different.

To assess this point, $PS-PVP_1$ and $PS-PVP_2$ were dissolved in ethanol and toluene, respectively, and dynamic light scattering experiments were performed on the solutions. In the case of $PS-PVP_1$ in ethanol, the PVP block has good solubility in the solvent, whereas the PS block has very poor miscibility. This leads to the formation of spherical micelles with a PS-rich core and PVP-rich corona, as shown by the dynamic light scattering correlation function (Figure 7) of a 0.2 wt % solution of $PS-PVP_1$ in ethanol at 25 °C. As shown in Figure 8, different concentrations were studied, and the results for the average micelle diameter were extrapolated to zero concentration. A limiting diameter of 110 nm has been obtained for the diameter of $PS-PVP_1$ micelles in ethanol at 25 °C. By using this value, it is possible to estimate the number of block copolymers forming one micelle, f, which may be considered as a first rough estimation of the tendency of the block copolymer to segregate. Following Vagberg et al.,[32] the radius of the micelle, R_m, can be calculated as

$$R_m = \left(\frac{8 N_S f^{(1-\nu)/2\nu}}{3 \cdot 4^{1/\nu} \nu} a_s^{1/\nu} + \left(\frac{3 N_C f}{4\pi\rho_C} \right)^{1/3\nu} \right)^{\nu}$$

where N_S is the number of monomers in each corona block, a_s is the statistical segment length, N_C is the number of monomers in the core, ρ_C is the number density of monomers in the core (normally taken as the bulk density of the incompatible block), and ν is the radius of gyration scaling exponent, equal to $^3/_5$ for good solvents and $^1/_2$ for Θ solvents. If we apply eq 1 to the $PS-PVP_1$ in ethanol, taking $^3/_5$ for ν, 0.67 nm for a_s,[33] and the measured value of 55 nm for R_m, a value of 243 is calculated for f. This value is rather high for such diluted solutions and indicates a very strong tendency for micelle formation of $PS-PVP_1$ in ethanol.

Dynamic light scattering experiments performed on $PS-PVP_2$ in toluene at 25 °C did not show any micelle formation, presumably, due to the greater solubility of PVP in toluene than PS in ethanol. Different annealing times were used to allow micelles to form, but no micelles were observed within a period of a month. New experiments were carried out for the same $PS-PVP_2$ system, but replacing toluene with cyclohexane. This solvent has a lower solubility parameter ($\delta = 8.2$ (cal/cm^3)$^{1/2}$) than toluene ($\delta = 8.9$ (cal/cm^3)$^{1/2}$), and therefore the solubility of PVP in this solvent should also decrease relative to that in toluene. However, because cyclohexane is a Θ solvent for PS at 34 °C, the experiments were performed at 50 °C to ensure good solubility of the PS block. At this temperature and in cyclohexane, micelles of $PS-PVP_2$ are observed, as is evident in the correlation function of the 0.2 wt % solution (see Figure 9a). However, an average micelle diameter of only 54 nm is measured for the above solution. The calculation of the exact number of chains forming a micelle is in this case more difficult, since the solvent is somewhat close to Θ conditions for PS, and the scaling exponent for the corona is unknown. Equation 1 can therefore provide only a rough indication of the upper limit in the number of chains per micelle, if the specific $^1/_2$ scaling exponent of Θ solutions is assumed for the corona. In this case f obtained by eq 1 is 27, which is much lower than the value of 243 for the $PS-PVP_1$ in ethanol. Although only a rough approximation for the number of chains per micelle can be obtained in this case, the number is expected to decrease rapidly with ν if R_m is maintained at the measured value of 27 nm, as shown in Figure 9b. Indeed, f rapidly decreases to such low values that the assumptions underlying the derivation of eq 1 are no longer valid. Evidently, it can be concluded that the population of chains in a micelle, and therefore the tendency of the block copolymer to segregate is much lower for $PS-PVP_2$ in cyclohexane at 50 °C than for $PS-PVP_1$ in ethanol at 25 °C.

Bearing this in mind, a 0.13/0.80/0.07 composition blend of $PS_1/PVP_2/PS-PVP_2$ blend was cast according to the usual procedure, but PS_1 and $PS-PVP_2$ were this time dissolved in cyclohexane at 50 °C and the 1:1 solution of PVP_2 in ethanol was added dropwise under continuous stirring. The solution turned white, indicating emulsification occurred with this choice of solvents. This is confirmed by the optical and TEM micrographs in parts a and b of Figure 10, respectively. However, PS inclusions within the PVP droplets were observed this time, confirming a more extended mixing compared to the previous high internal phase emulsions in Figure 3. The above observations lead to the following conclusions: (i) an emulsification leading to polyHIPE morphologies will occur only when the block copolymer has a tendency to segregate strongly enough to form micelles in solution with its respective selective solvent; (ii) the morphology of the final polyHIPE and the degree of

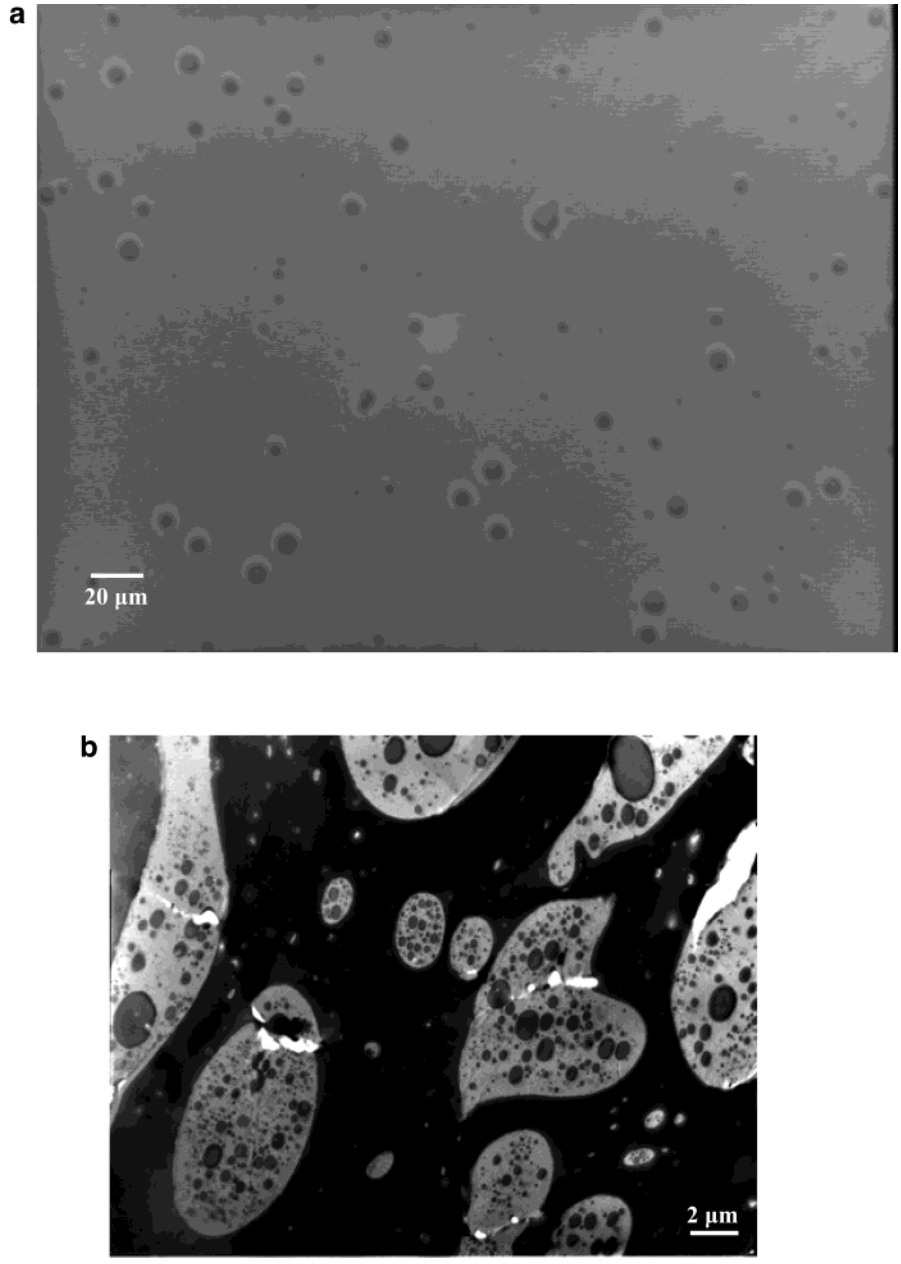

Figure 6. Optical **(**a**)** and TEM **(**b**)** micrographs of a $PS_1/PVP_2/PS-PVP_2$ blend of composition by volume: 0.13/0.80/0.07 obtained by using toluene as a solvent for PS plus $PS-PVP_2$ and ethanol for PVP.

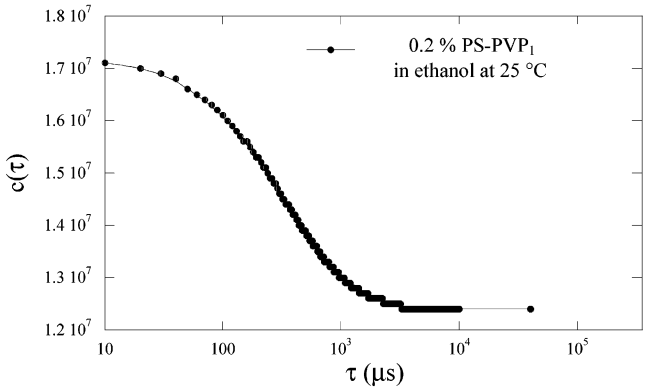

Figure 7. Dynamic light scattering correlation function of a 0.2 wt % solution of $PS-PVP_1$ in ethanol at 25 °C.

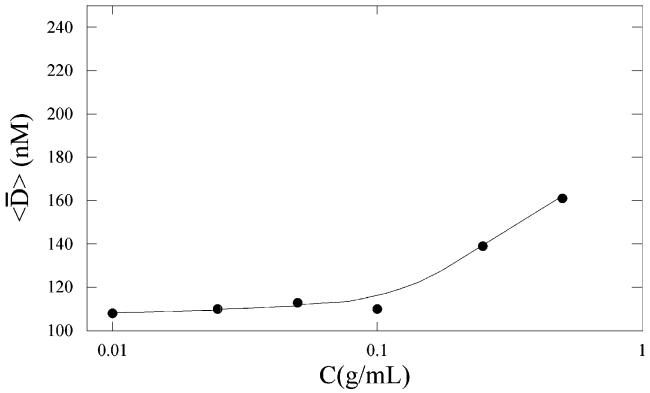

Figure 8. Measured diameter of $PS-PVP_1$ micelles in ethanol at 25 °C as a function of solution concentration. The results extrapolated to zero concentration give a limiting value of the diameter of 110 nm.

mixing of different components are related to the driving force for the formation of micelles. Thermodynamic arguments can be invoked to quantify such a driving force and provide a useful explanation of the experimental trends observed.

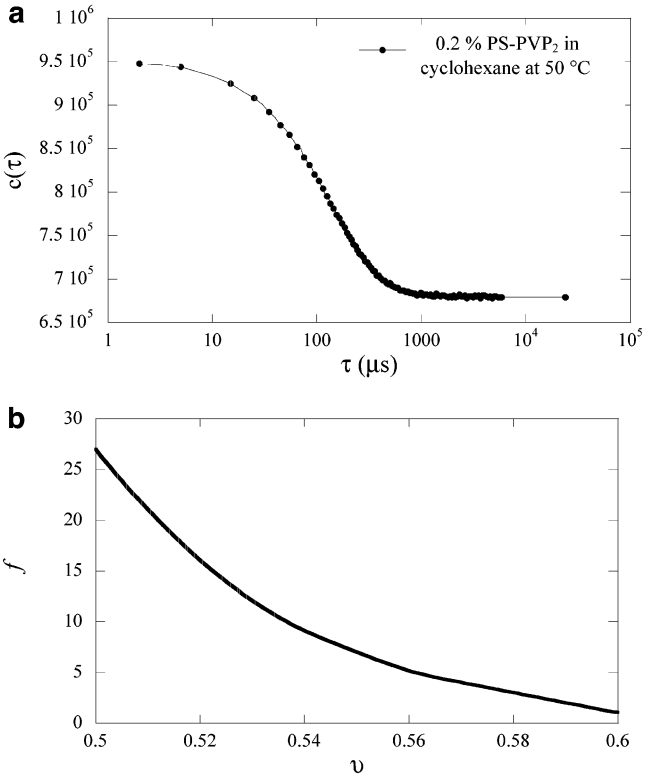

Figure 9. (a) Dynamic light scattering correlation function of a 0.2 wt % solution of PS−PVP_2 in cyclohexane at 50 °C. **(**b**)** Variation of the population of chains per micelle as a function of the scaling exponent ν according to eq 1 for PS−PVP_2 in cyclohexane at 50 °C.

The driving force for segregation of the block copolymer to the interface primarily reflects the excess free energy of the unfavorable block in the solvent. Per molecule, this is approximately equal to the difference between the chemical potential of the block copolymer at the interface and that of an unaggregated block copolymer dissolved in the solvent. This difference is thus provided by the differences in the chemical potential of the unfavorable block, $\Delta\mu_{us}$, since less significant changes occur for the favorable block when the block copolymer is dissolved or segregated at the interface. Following the lines of thought of previous work,[34] this variation can be expressed as

$$\Delta\mu_{us} \approx RTN_u(\chi_{up} - \chi_{ug})\phi^2 \quad (2)$$

where R is the perfect gas constant, T is the absolute temperature, N_u is the number of units of the unfavorable block, χ_{up} and χ_{ug} are the Flory interaction parameters between the unfavorable block unit and the poor solvent, and the unfavorable block unit and the good solvent, respectively, and ϕ is the volume fraction of the solvent. For very dilute conditions in a good solvent we can assume that χ_{ug} and ϕ are equal to 0 and 1, respectively, and therefore

$$\Delta\mu_{us} \approx RTN_u\chi_{up} \quad (3)$$

This contribution, if large enough, drives micelles to form and provides a strong driving force for segregation to the interface. Micelles tend to form when the chemical potential exceeds a certain critical value. Past that threshold the chemical potential increases only slightly with block copolymer concentration, and thus the critical chemical potential constitutes the maximum driving force for the block copolymer to segregate to the interface. If the solvent is a bit less poor for the core block, i.e., χ_{up} decreases, the chemical potential of the block copolymer in the solution is less than needed for good segregation, and block copolymer cannot stabilize the interface. To evaluate the differences in chemical potential in the three cases investigated, we can make use of the well-known expression from regular solution theory expressing the Flory interaction parameter in terms of the solubility parameters:

$$\chi_{us} = (V_u/RT)(\delta_u - \delta_s)^2 \quad (4)$$

where δ_u and δ_s are the solubility parameters of the unfavorable block and the poor solvent, respectively, and V_u is the repeat unit molar volume of the polymer used for solubility parameter calculation. Therefore, the driving force for block copolymer segregation at the interface, $\Delta\mu_{us}$, can be estimated by

$$\Delta\mu_{us} \approx N_u V_u(\delta_u - \delta_s)^2 \quad (5)$$

Table 2 summarizes the values of $\Delta\mu_{us}$ as calculated by eq 5 for the three solutions investigated in the present work. These results support the arguments discussed above and quantify the driving force for segregation of the block copolymer at the interface, PS−PVP_1 in ethanol as having the highest chemical potential, followed by PS−PVP_2 in cyclohexane and PS−PVP_2 in toluene.

Finally, we note that at these semidilute concentrations the kinetics of segregation of block copolymer is expected to be rapid for both dissolved block copolymers and block copolymer micelles. Therefore, unlike the bulk melt case where formation of micelles is detrimental for segregation kinetics to the interface, in the present case, the kinetics of micelle formation does not inhibit a rapid stabilization of the interfaces, and the quality of the block copolymer as surfactant is primarily dependent on its chemical potential.

Summary

We have investigated the interfacial curvature in a model PS/PVP/PS−PVP blend system under equilibrium and nonequilibrium conditions. Simulations based on self-consistent-field theory predict the curvature of the interface to be a function of blend composition and block copolymer asymmetry. These simulations constitute valuable input for understanding morphology development in the model system, where nonequilbrium effects are more pronounced. PS/PVP/PS−PVP blends with composition, molecular weight, and block copolymer asymmetry analogous to those used in the simulations were produced by solvent casting. In one case, a common solvent was used for PS and PVP, leading to intimate mixing of molecules and a final morphology developing by nucleation and growth upon solvent removal. For high volume fraction of one of the two homopolymers, the morphology and interfacial curvature observed experimentally were in agreement with the numerical simulations, the minority phase being dispersed in the majority phase and thereby approaching a local minimum of the total interfacial energy. However, when selective solvents were used for PS and PVP during solvent casting, the final morphology de-

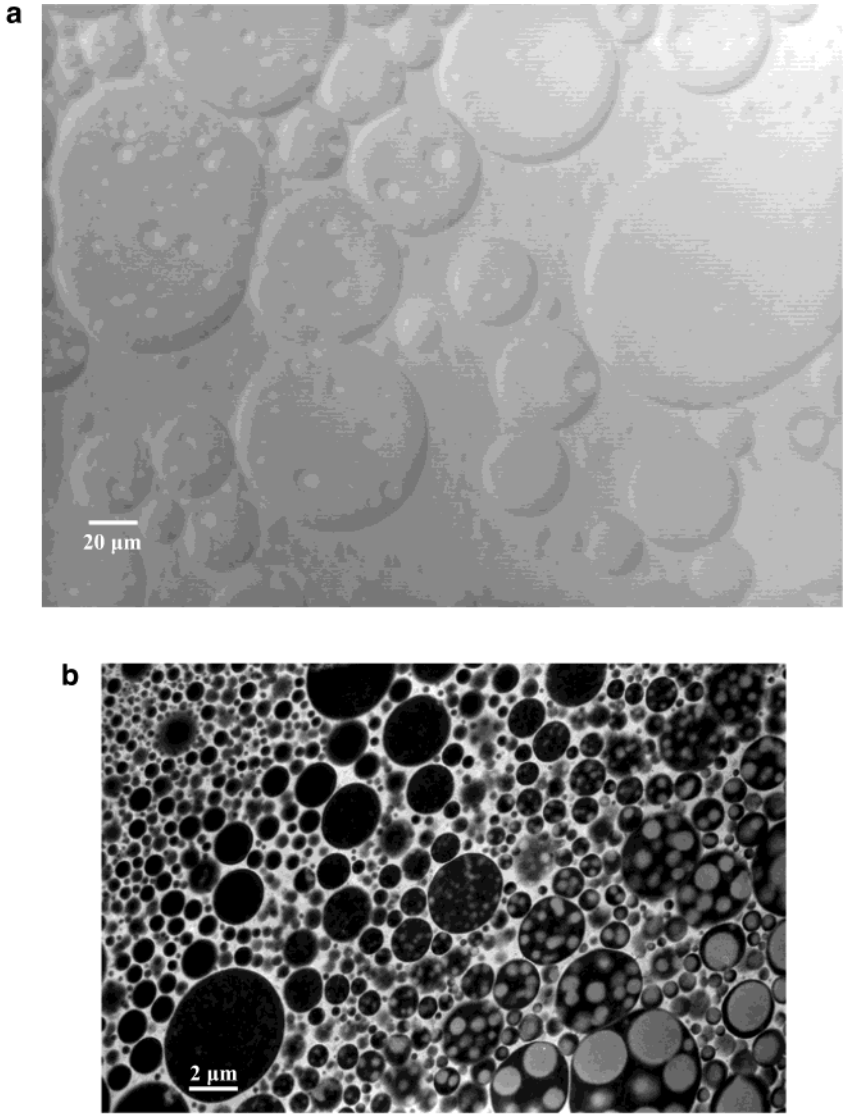

Figure 10. Optical **(**a**)** and TEM **(**b**)** micrographs of polyHIPE at compositions of 0.13/0.80/0.07 as obtained from solvent casting at 50 °C, using ethanol as solvent for PVP and cyclohexane for PS plus PS−PVP_2.

Table 2. Solubility Parameters, Number of Unfavorable Block Units, Block Copolymer Repeat Unit Volume, and Chemical Potentials Values As Calculated by Eq 5, for the Different Solutions Investigated

	δ_u (cal/cm^3)$^{1/2}$	δ_s (cal/cm^3)$^{1/2}$	N_u	V_u (cm^3/mol)	$\Delta\mu_{us}$ (kcal/mol)
PS−PVP_1 in ethanol	9.3	12.7	108	100	125
PS−PVP_2 in cyclohexane	10.7	8.2	138	101	87
PS−PVP_2 in toluene	10.7	8.9	138	101	45

veloped through an intermediate emulsion phase. After solvent removal, this technique proved to be a valuable procedure for producing polyHIPE blends, with the continuous phase having a volume fraction as low as 13%. The conditions for which the emulsification process occurs were assessed by dynamic light scattering, and it was shown that in order to produce polyHIPE morphologies the block copolymer in the solution needs to have such a strong chemical potential that micelles are formed. Thermodynamic arguments were presented to support this experimental evidence.

Acknowledgment. PolyE Incorporated is gratefully acknowledged for financial support. This work made use of MRL central facilities supported by the National Science Foundation under Award DMR 00-80034.

References and Notes

(1) Jones, R. A. L.; Richards, R. W. *Polymers at Surfaces and Interfaces*; Cambridge University Press: Cambridge, MA, 1999.
(2) Utracki, L. A. *Polymers Alloys and Blends, Thermodynamics and Rheology*; Hanser Publishers: Munchen, 1989.
(3) Broseta, D.; Fredrickson, G. H.; Helfand, E.; Leibler, L. *Macromolecules* **1990**, *23*, 132.
(4) Govorun, E. N.; Erukhimovich, I. *Langmuir* **1999**, *15*, 8392.
(5) Dan, N.; Tirrell, M. *Macromolecules* **1993**, *24*, 637.
(6) Wang, Z. G.; Safran, S. A. *J. Chem. Phys.* **1991**, *94*, 679.
(7) Leermakers, F. A. M.; vanNoort, J.; Oversteegen, S. M.; Barneveld, P. A.; Lyklema, J. *Faraday Discuss.* **1996**, *104*, 317.
(8) Lissant, K. J. *J. Colloid Interface Sci.* **1966**, *22*, 462.
(9) Lissant, K. J.; Mayhan, K. G. *J. Colloid Interface Sci.* **1973**, *42*, 201.
(10) Princen, H. M. *J. Colloid Interface Sci.* **1979**, *71*, 55.
(11) Westesen, K.; Wehler, T. *Colloids Surf., A* **1993**, *78*, 125.

(12) Groeneweg, F.; Vandieren, F.; Agterof, W. G. M. *Colloids Surf., A* **1994**, *91*, 207.
(13) Kunieda, H.; Fukui, Y.; Uchiyama, H.; Solans, C. *Langmuir* **1996**, *12*, 2136.
(14) Ozawa, K.; Solans, C.; Kunieda, H. *J. Colloid Interface Sci.* **1997**, *188*, 275.
(15) Mork, S. W.; Rose, G. D.; Green, D. P. *J. Surfactants Deterg.* **2001**, *4*, 127.
(16) Haney, P.; Huxham, I. M.; Rowatt, B.; Sherrington, D. C.; Tetley, L. *Macromolecules* **1991**, *24*, 117.
(17) Sherrington, D. C. *Makromol. Chem. Symp.* **1991**, *70*, 303.
(18) Cameron, N. R.; Sherrington, D. C. *J. Chem. Soc., Faraday Trans.* **1996**, *92*, 1543.
(19) Cameron, N. R.; Sherrington, D. C. *Macromolecules* **1997**, *30*, 5860.
(20) Cameron, N. R.; Barbetta, A. *J. Mater. Chem.* **2000**, *10*, 2466.
(21) Tai, H.; Sergienko, A.; Silverstein, M. S. *Polymer* **2001**, *42*, 4473.
(22) Tai, H.; Sergienko, A.; Silverstein, M. S. *Polym. Eng. Sci.* **2001**, *41*, 1540.
(23) Bhumgara, Z. *Filtr. Sep.* **1995**, *32*, 245.
(24) Benicewicz, B. C.; Jarvinen, G. D.; Kathios, D. J.; Jorgensen, B. S. *J. Radioanal. Nucl. Chem.* **1998**, *235*, 31.
(25) Busby, W.; Cameron, N. R.; Jahoda, C. A. B. *Biomacromolecules* **2001**, *2*, 154.
(26) Dautzenberg, H.; Dautzenberg, H.; Gensrich, H. J.; Grobe, V.; Hicke, H. G.; Paul, D. *Acta Polym.* **1989**, *40*, 177.
(27) Albrecht, W.; Klug, P.; Makschin, W.; Weigel, T.; Gensrich, H. J.; Grobe, V.; Paul, D. *Acta Polym.* **1992**, *43*, 165.
(28) Gajnos, G. E.; Lu, D.; Karasz, F. E. *Macromolecules* **1976**, *9*, 551.
(29) Foldes, E.; Fekete, E.; Karasz, F. E.; Pukanszky, B. *Polymer* **2000**, *41*, 975.
(30) Yokoyama, H.; Kramer, E. J. *Macromolecules* **1998**, *31*, 7871.
(31) Drolet, F.; Fredrickson, G. H. *Phys. Rev. Lett.* **1999**, *83*, 4317.
(32) Vagberg, L. J. M.; Cogan, K. A.; Gast, P. A. *Macromolecules* **1991**, *24*, 1670.
(33) Fetters, L. J.; Lohse, D. J.; Richter, D.; Witten, T. A.; Zirkel, A. *Macromolecules* **1994**, *27*, 4639.
(34) Shull, K. R.; Kramer, E. J. *Macromolecules* **1990**, *23*, 4769.

MA021196L